MecSol2013
International Symposium on Solid Mechanics
April 18-19, 2013
Porto Alegre, Rio Grande do Sul, Brazil

Elastodynamic analysis by optimized FEM-BEM iterative coupling procedures – a frequency domain approach

Delfim Soares Jr.
Structural Engineering Department
Federal University of Juiz de Fora
delfim.soares@ufjf.edu.br

Kleber A. Gonçalves
Department of Civil Engineering
Federal University of Rio de Janeiro
kleber@coc.ufrj.br

José Claudio de Faria Telles
Department of Civil Engineering
Federal University of Rio de Janeiro
telles@coc.ufrj.br

ABSTRACT

This paper presents a coupled FEM-BEM strategy for the numerical analysis of elastodynamic problems where infinite-domain models and complex heterogeneous media are involved, rendering a configuration in which neither the Finite Element Method (FEM) nor the Boundary Element Method (BEM) is most appropriate for the numerical analysis. In this case, the coupling of these methodologies is recommended, allowing exploring their respective advantages. Here, frequency domain analyses are focused and an iterative FEM-BEM coupling technique is considered. In this iterative coupling, each sub-domain of the model is solved separately, and the variables at the common interfaces are iteratively renewed, until convergence is achieved. A relaxation parameter is introduced into the coupling algorithm and an expression for its optimal value is deduced. Optimal relaxation parameters are computed in order to ensure the convergence of the iterative procedure, properly dealing with the frequency domain wave propagation ill-posed problem. The iterative FEM-BEM coupling technique allows independent discretizations to be efficiently employed for both finite and boundary element methods, without any requirement of matching nodes at the common interfaces. Moreover, it leads to smaller and better-conditioned systems of equations (different solvers, suitable for each sub-domain, may be employed), which do not need to be treated (inverted, triangularized etc.) at each iterative step, providing an accurate and efficient methodology.

Keywords: Elastodynamics; Frequency Domain; Iterative Coupling; Relaxation Parameter.

1 INTRODUCTION

Standard coupling of FEM/BEM procedures can lead to several problems with respect to efficiency, accuracy and flexibility. First, the coupled system of equations has a banded symmetric structure only in the FEM part, while in the BEM part it is non-symmetric and fully populated. Consequently, for its solution, the optimized solvers usually used by the FEM cannot be employed anymore, which leads to rather expensive calculations with respect to computer time. Second, quite different physical properties may be involved in the coupled model, resulting in bad-conditioned

matrices when standard coupling procedures are considered. This may affect the accuracy of the methodology, providing misleading results. Third, the standard coupling methodology does not allow independent discretization for each sub-domain of the model, requiring matching nodes at common interfaces, which drastically affects the flexibility and versatility of the technique.

In order to evade these drawbacks, iterative coupling procedures have been developed, mostly taking into account time domain interacting models [1-3]. Iterative coupling approaches allow BEM and FEM sub-domains to be analysed separately, leading to smaller and better-conditioned systems of equations (different solvers, suitable for each sub-domain, may be employed). Moreover, a small number of iterations is required for the algorithm to converge and the matrices related to the smaller governing systems of equations do not need to be treated (inverted, triangularized etc.) at each iterative step, providing an efficient methodology. This coupling technique allows independent discretizations to be efficiently employed for the boundary and finite element sub-domains, without any requirement of matching nodes at the common interfaces. As a matter of fact, in the present work, constant boundary elements and linear finite elements are considered, and matching functional nodes are never provided in the common interfaces. It is important to observe, however, that frequency domain analyses usually give rise to ill-posed problems and, in these cases, the convergence of the iterative coupling algorithm can be either too slow or unachievable if no special procedure is taken into account. In order to deal with this ill-posed problem and ensure convergence of the iterative coupling algorithm, an optimal iterative procedure is adopted here, with optimal relaxation parameters being computed at each iterative step. Thus, an expression to compute optimal relaxation parameters, which is quite efficient and easy to implement, is provided and discussed, being its effectiveness illustrated at the end of the paper, where numerical examples are analyzed. In the numerical examples, soil-structure interacting models are discussed, being the results of the proposed iterative coupling formulation compared to those of the standard coupling technique. As one will observe, the proposed technique is flexible, robust and efficient, allowing a quite effective coupling of the finite element and boundary element methods for frequency domain elastodynamic analyses.

2 GOVERNING EQUATIONS

The frequency domain elastic wave equation for homogenous media is given by:

$$\rho(c_d^2 - c_s^2)u_j(X,\omega)_{,ji} + \rho c_s^2 u_i(X,\omega)_{,jj} + (\omega^2\rho - i\omega\nu)u_i(X,\omega) + b_i(X,\omega) = 0 \qquad (1)$$

where $u_i(X,\omega)$ and $b_i(X,\omega)$ stand for the displacement and the body force distribution components, respectively. In Equation (1), c_d is the dilatational wave velocity and c_s is the shear wave velocity, they are given by: $c_d^2 = (\lambda + 2\mu)/\rho$ and $c_s^2 = \mu/\rho$, where ρ is the mass density and λ and μ are the Lamé's constants. ν stands for viscous damping related parameters. Equation (1) can be obtained from the combination of the following basic mechanical equations (proper to model heterogeneous media):

$$\sigma_{ij}(X,\omega)_{,j} + \big(\rho(X)\omega^2 - i\omega\nu(X)\big)u_i(X,\omega) + b_i(X,\omega) = 0 \qquad (2a)$$
$$\sigma_{ij}(X,\omega) = \lambda(X)\delta_{ij}\varepsilon_{kk}(X,\omega) + 2\mu(X)\varepsilon_{ij}(X,\omega) \qquad (2b)$$
$$\varepsilon_{ij}(X,\omega) = (1/2)(u_i(X,\omega)_{,j} + u_j(X,\omega)_{,i}) \qquad (2c)$$

where $\sigma_{ij}(X,\omega)$ and $\varepsilon_{ij}(X,\omega)$ are, respectively, stress and strain tensor components, and δ_{ij} is the Kronecker delta ($\delta_{ij} = 1, \text{for } i = j \text{ and } \delta_{ij} = 0, \text{for } i \neq j$) . Equation (2a) is the momentum equilibrium equation; Equation (2b) represents the constitutive law of the linear elastic model and

Equation (2c) stands for kinematical relations. The boundary conditions of the elastodynamic problem are given by:

$$u_i(X,\omega) = \bar{u}_i(X,\omega) \text{ for } X \in \Gamma_1 \quad (3a)$$
$$\tau_i(X,\omega) = \sigma_{ij}(X,\omega)n_j(X) = \bar{\tau}_i(X,\omega) \text{ for } X \in \Gamma_2 \quad (3b)$$

where the prescribed values are indicated by over bars, $\tau_i(X,\omega)$ denotes the traction vector along the boundary and $n_j(X)$ stands for the components of the unit outward normal vector.

3 BOUNDARY ELEMENT MODELLING

The BEM integral equation related to the elastodynamic model is given by:

$$c_{ij}(\xi)u_j(\xi,\omega) = \int_\Gamma u^*_{ij}(X;\xi,\omega)\tau_j(X,\omega)\,d\Gamma - \int_\Gamma \tau^*_{ij}(X;\xi,\omega)\,u_j(X)\,d\Gamma + \varsigma_i(X;\xi,\omega) \quad (4)$$

where $c_{ij}(\xi)$ depends on geometric aspects, $\varsigma_i(X;\xi,\omega)$ stands for possible domain integral contributions (such as body sources) and the terms $u^*_{ij}(X;\xi,\omega)$ and $\tau^*_{ij}(X;\xi,\omega)$ represent the fundamental displacement and traction, respectively (X is the field point and ξ is the source point). For a two-dimensional approach, the fundamental solutions can be found at [4].

By introducing spatial approximations for the variables of the model into the integral Equation (4), the following system of equations can be obtained, once proper numerical treatment is considered [4]:

$$\boldsymbol{C}\boldsymbol{U}(\omega) = \boldsymbol{G}(\omega)\boldsymbol{T}(\omega) - \boldsymbol{H}(\omega)\boldsymbol{U}(\omega) + \boldsymbol{S}(\omega) \quad (5)$$

where $\boldsymbol{C}$, $\boldsymbol{G}$ and $\boldsymbol{H}$ are influence matrices, $\boldsymbol{S}$ is a vector related to domain integrals and $\boldsymbol{U}$ and $\boldsymbol{T}$ are displacement and traction vectors, respectively, at frequency ω. After considering the boundary conditions of the problem (translating all the known variables to the right-hand-side of Equation (5), and the unknown fields to the left-hand-side), the BEM responses for the elastic model can be computed for the given frequency ω.

4 FINITE ELEMENT MODELLING

The integral weak-form of the governing equations at section 2 can be written as:

$$-\omega^2 \int_\Omega \rho(X)u_i(X,\omega)w_{ik}(X)d\Omega + i\omega \int_\Omega \nu(X)u_i(X,\omega)w_{ik}(X)d\Omega +$$
$$+ \int_\Omega \sigma_{ij}(X,\omega)w_{ik}(X)_{,j}d\Omega + \int_\Omega b_i(X,\omega)w_{ik}(X)d\Omega - \int_{\Gamma_2} \tau_i(X,\omega)w_{ik}(X)d\Gamma = 0 \quad (6)$$

where $w_{ik}(X)$ stands for a weight function, which is assumed to have null values in the essential boundary (i.e., $w_{ik}(X) = 0$ for $X \in \Gamma_1$).

By introducing spatial approximations for the variables of the model into the integral Equation (6), and by adopting these approximations to define the specified weight functions (Galerkin Method), the following system of equations can be obtained, once proper numerical treatment is considered [5-6]:

$$-\omega^2\boldsymbol{M}\boldsymbol{U}(w) + i\omega\boldsymbol{C}\boldsymbol{U}(\omega) + \boldsymbol{K}\boldsymbol{U}(\omega) = \boldsymbol{F}(\omega) \quad (7)$$

where $\boldsymbol{M}$, $\boldsymbol{C}$ and $\boldsymbol{K}$ stand for the mass, damping and stiffness matrix of the model, respectively, and $\boldsymbol{U}$ and $\boldsymbol{F}$ stand for the nodal displacement and force vector, respectively. Matrices $\boldsymbol{M}$, $\boldsymbol{C}$ and $\boldsymbol{K}$ are computed taking into account the first, second and third terms in Equation (6), respectively, whereas vector $\boldsymbol{F}$ is computed taking into account the last two terms in the l.h.s. of Equation (6) (for the stiffness matrix computation, equations (2b-c) are employed to relate the stress tensor with the displacement vector). After considering the boundary conditions of the problem, the FEM responses for the elastodynamic model can be computed for the given frequency ω, taking into account Equation (7).

5 COUPLING PROCEDURES

In order to enable the coupling between the BEM and the FEM sub-domains of the model, an iterative procedure is employed here, which performs a successive renewal of the relevant variables at the common interfaces. The proposed approach is based on the imposition of prescribed displacement at the BEM sub-domain and of prescribed nodal forces at the FEM sub-domain. Since the two sub-domains are analysed separately, the relevant systems of equations are formed independently, before the iterative process starts, and are kept constant for each frequency along the iterative process. The separate treatment of the two sub-domains allows independent discretizations to be used on both parts, without any special requirement of matching nodes along the common interfaces. Thus, the coupling algorithm can be presented for a generic case, in which the interface nodes may not match, allowing exploiting this benefit of the iterative coupling formulation.

To ensure and/or to speed up convergence, a relaxation parameter λ is introduced in the iterative coupling algorithm. The effectiveness of the iterative process is strongly related to the selection of this relaxation parameter, since an inappropriate selection for λ can significantly increase the number of iterations in the analysis or, even worse, make convergence unfeasible. At the end of the section, an optimal relaxation parameter is calculated, taking into account the coupled BEM-FEM frequency-domain formulation.

5.1 Iterative coupling procedures

Initially, in the k^{th} iterative step of the FEM-BEM coupling, the FEM sub-domain is analysed and the structure displacements at the common interfaces ${}_f\boldsymbol{U}_I^{(k)}(\omega)$ (subscript I indicates the common interface, whereas f and b indicates finite and boundary element sub-domains, respectively) are computed, as described in section 4. In this case, ${}_f\boldsymbol{U}_I^{(k)}(\omega)$ is evaluated taking into account prescribed nodal forces at the common interfaces ${}_f\boldsymbol{F}_I^{(k)}$, which are provided from the previous iterative step (in the first iterative step, null prescribed nodal forces are considered). Once ${}_f\boldsymbol{U}_I^{(k)}(\omega)$ is computed, it is applied to evaluate the essential boundary conditions that are prescribed at the common interfaces of the BEM sub-domains. More precisely, ${}_f\boldsymbol{U}_I^{(k)}(\omega)$ is used to compute BEM displacements, as indicated below:

$$ {}_b\boldsymbol{U}_I^{(k+\lambda)}(\omega) = \int_{\Gamma_I} \boldsymbol{\delta}^T(X - {}_bX)\ {}_f\boldsymbol{N}(X) d\Gamma\ {}_f\boldsymbol{U}_I^{(k)}(\omega) \tag{8} $$

where $\boldsymbol{\delta}$ stands for a matrix representation of the Dirac's Delta function, employed here just to properly indicate the computation of the variables at the BEM nodes ${}_bX$, and $\boldsymbol{N}(X)$ stands for the BEM or FEM interpolation functions, according to the subscript b or f, respectively.

To better describe the proposed FEM-BEM coupling methodology, Figure 1 illustrates its application for the case of constant boundary elements and linear triangular finite elements.

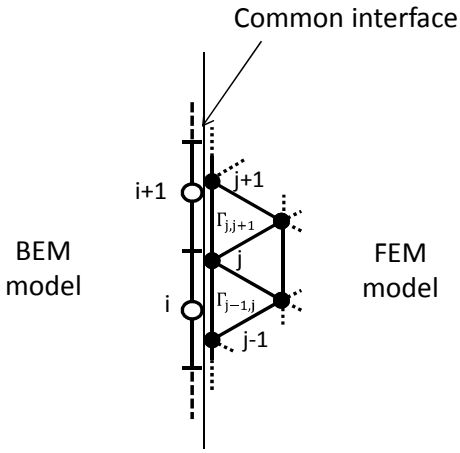

Figure 1: Detail of a portion of the FEM-BEM interface when linear triangular finite elements and constant boundary are used. In the figure, $j-1$, j and $j+1$ are FEM interface nodes, while i and $i+1$ are BEM nodes. Displacements at BEM node i can be computed by interpolation of FEM displacements at nodes $j-1$ and j (Equation (8)); FEM nodal force in j can be calculated by integration of the traction along boundaries $\Gamma_{j-1,j}$ and $\Gamma_{j,j+1}$, using Equation (10) and considering FEM linear and BEM piecewise constant shape functions along these boundaries.

As previously discussed, in this work, relaxation parameters are considered in order to ensure and/or to speed up the convergence of the iterative process. Thus, the displacements ${}_b\boldsymbol{U}_I^{(k+\lambda)}$ that are calculated by Equation (8) are actualized as follow:

$$ {}_b\boldsymbol{U}_I^{(k+1)}(\omega) = (\lambda)\ {}_b\boldsymbol{U}_I^{(k+\lambda)}(\omega) + (1-\lambda)\ {}_b\boldsymbol{U}_I^{(k)}(\omega) \tag{9}$$

where λ stands for the relaxation parameter.

Once the BEM displacements at the common interfaces are computed, the BEM sub-domains can be analyzed, as described in section 3. As a consequence, the BEM tractions at the common interfaces are evaluated ${}_b\boldsymbol{T}_I^{(k+1)}$, allowing the computation of the natural boundary conditions that are prescribed at the FEM sub-domains at the next iterative step. This is carried out as indicated below:

$$ {}_f\boldsymbol{F}_I^{(k+1)}(\omega) = \int_{\Gamma_I} {}_f\boldsymbol{N}^T(X)\ {}_b\boldsymbol{N}(X) d\Gamma\ {}_b\boldsymbol{T}_I^{(k+1)}(\omega) \tag{10}$$

Once ${}_f\boldsymbol{F}_I^{(k+1)}(\omega)$ is computed, the algorithm goes on to the next iterative step, repeating all the above described procedures, until convergence is achieved.

As it is illustrated in section 6, a proper selection for λ at each iterative step is extremely important for the effectiveness of the iterative coupling procedure. In order to obtain an easy to implement, efficient and effective expression for the relaxation parameter computation, in the next sub-section optimal λ values are deduced.

5.2 Optimal relaxation parameter

In order to evaluate an optimal relaxation parameter, the following square error functional is minimized here:

$$f(\lambda) = \left\| {}_b\boldsymbol{U}_I^{(k+1)}(\lambda) - {}_b\boldsymbol{U}_I^{(k)}(\lambda) \right\|^2 \tag{11}$$

where ${}_b\boldsymbol{U}_I$ stands for the BEM prescribed values at the common interfaces.

Taking into account the relaxation of the prescribed values for the (*k+1*) and (*k*) iterations, Equations (12a) and (12b) may be written, based on the definition in Equation (9):

$${}_b\boldsymbol{U}_I^{(k+1)} = (\lambda)\ {}_b\boldsymbol{U}_I^{(k+\lambda)} + (1-\lambda)\ {}_b\boldsymbol{U}_I^{(k)} \tag{12a}$$

$${}_b\boldsymbol{U}_I^{(k)} = (\lambda)\ {}_b\boldsymbol{U}_I^{(k+\lambda-1)} + (1-\lambda)\ {}_b\boldsymbol{U}_I^{(k-1)} \tag{12b}$$

Substituting Equations (12) into Equation (11) yields:

$$\begin{aligned} f(\lambda) &= \left|\left|(\lambda)\boldsymbol{W}^{(k+\lambda)} + (1-\lambda)\ \boldsymbol{W}^{(k)}\right|\right|^2 = \\ &= (\lambda^2)\left|\left|\boldsymbol{W}^{(k+\lambda)}\right|\right|^2 + 2\lambda(1-\lambda)\left(\boldsymbol{W}^{(k+\lambda)}, \boldsymbol{W}^{(k)}\right) + (1-\lambda)^2\left|\left|\boldsymbol{W}^{(k)}\right|\right|^2 \end{aligned} \tag{13}$$

where the inner product definition is employed (e.g., $(\boldsymbol{W}, \boldsymbol{W}) = \|\boldsymbol{W}\|^2$) and new variables, as defined in Equation (14), are considered.

$$\boldsymbol{W}^{(k+\lambda)} = {}_b\boldsymbol{U}_I^{(k+\lambda)} - {}_b\boldsymbol{U}_I^{(k+\lambda-1)} \tag{14}$$

To find the optimal λ that minimizes the functional $f(\lambda)$, Equation (13) is differentiated with respect to λ and the result is set to zero, as described below:

$$\lambda\left\|\boldsymbol{W}^{(k+\lambda)}\right\|^2 + (1-2\lambda)\left(\boldsymbol{W}^{(k+\lambda)}, \boldsymbol{W}^{(k)}\right) + (\lambda-1)\left\|\boldsymbol{W}^{(k)}\right\|^2 = 0 \tag{15}$$

Re-arranging the terms in equation (15), yields:

$$\lambda = \frac{\left(\boldsymbol{W}^{(k)}, \boldsymbol{W}^{(k)} - \boldsymbol{W}^{(k+\lambda)}\right)}{\left\|\boldsymbol{W}^{(k)} - \boldsymbol{W}^{(k+\lambda)}\right\|^2} \tag{16}$$

which is an easy to implement expression that provides an optimal value for the relaxation parameter λ, at each iterative step. This expression requires a low computational cost, when compared to other alternatives that can be found in the literature (see, for instance, [7]).

Additionally, one should keep in mind that the computed relaxation parameter is a complex number, since the problem is formulated in the frequency domain. This complex number computation could be ranged (e.g., imposing $|\lambda| \leq 1$), but the authors have observed that faster convergence is usually achieved in the iterative process if a non-restricted relaxation parameter selection, provided by Equation (16), is considered. Moreover, although the authors found that the iterative process is relatively insensitive to the value of the relaxation parameter used for the first step, in all the cases discussed here, a real value of $\lambda = 0.5$ is considered.

6 NUMERICAL ANALYSES

In order to illustrate the performance and potentiality of the discussed techniques, two application examples are considered here, corresponding to a circular ring-shaped structure involved by an infinite soil domain. Different material properties, as well as prescribed load/displacement configurations, are considered in the analyses.

6.1 Ring-shaped structure inside an infinite elastic domain

Consider a circular homogeneous ring-shaped elastic inclusion, inside a homogeneous and infinite elastic environment (see Figure 2a). The external environment has a density of $7{,}85 \times 103$ kg/m3, Young's modulus of $20{,}58 \times 1010$ N/m2 and Poisson's ratio of 0.2 (no damping is considered). This elastic material allows dilatational and shear waves to travel at 5397,17 m/s and 3305,08 m/s, respectively. The circular inclusion has an external radius of 3.0 m and an internal radius of 2.0 m and is made of the same elastic material of the external domain.

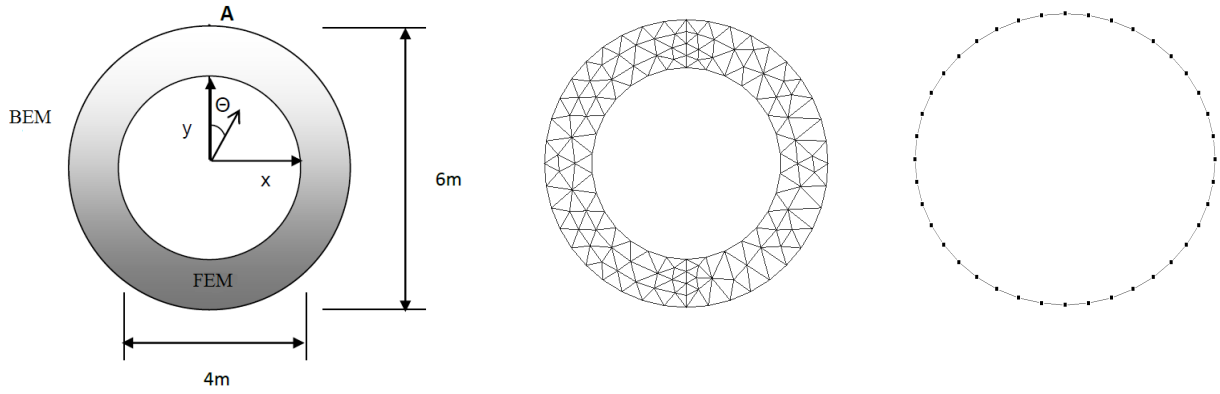

(a) (b) (c)

Figure 2: (a) sketch of the model; (b) FEM discretization; (c) BEM discretization.

The external environment is discretized by boundary elements distributed uniformly along the common interface (straight boundary elements with constant interpolation functions are adopted); the ring structure is modeled by using linear triangular finite elements. Fundamental harmonic displacements are prescribed at the internal cavity of the ring structure, which are acquired by considering a horizontal Dirac's delta force acting at the centre of the cavity. Thus, the analytical solution for the problem is known and it is provided by the model's fundamental solutions.

First, the external environment is modeled using 40 boundary elements, while a total of 210 elements (40 nodes at the interface) are considered at the finite element mesh. The corresponding FEM and BEM discretizations are illustrated in Figure 2b and 2c, respectively.

Figure 3 illustrates the displacements computed at point A (see Figure 2a), taking into account the proposed iterative coupling procedure, considering a frequency range from 100 to 5000 Hz. Analytical answers and results computed taking into account a standard FEM-BEM direct coupling methodology are also depicted in Figure 3, for comparison. As one can observe, the results provided by these different approaches are in good agreement. It is important to highlight that the coupled FEM-BEM results get closer to the analytical answers as the discretization of the model is refined.

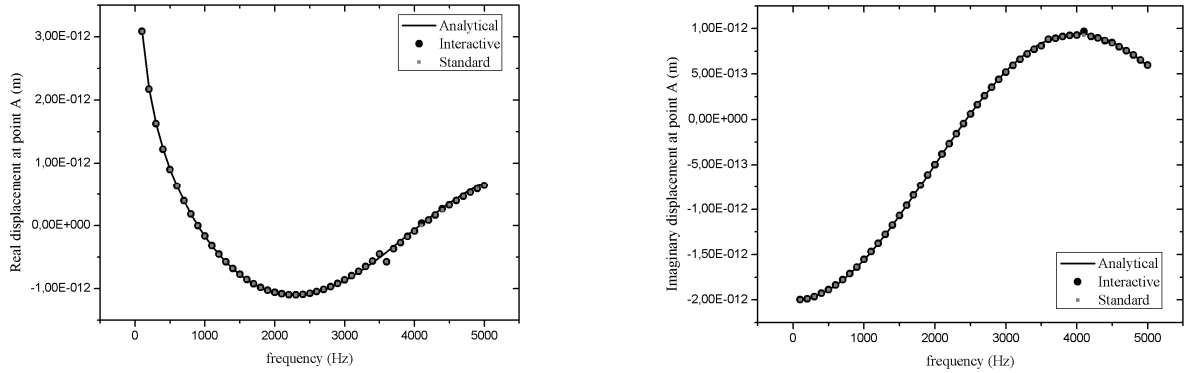

(a) (b)

Figure 3: Vertical displacements at point A: (a) real part; (b) imaginary part.

As a matter of fact, the convergence of the proposed technique is analyzed next, taking into account independent discretizations (and, as a consequence, no matching nodes at the common interface) for the FEM and the BEM. In order to do so, 4 discretizations for the BEM sub-domain and 4 discretizations for the FEM sub-domain are focused, as described in Table 1 (as one may observe, Meshes 2 are those depicted in Figure 2). These different discretizations are combined among each other and the errors that arise (taking into account the analytical answer of the model) are depicted in Figure 4. Three combinations are considered here, the first one considers the FEM mesh 4 (i.e., 160 nodes on the FEM common interface) combined with all the focused BEM meshes. This combination is referred here as "FEM 160 - BEM". The second combination considers the BEM mesh 4 (i.e., 160 nodes on the BEM common interface) combined with all the focused FEM meshes. This combination is referred here as "BEM 160 - FEM". Finally, standard node to node combinations (i.e., considering matching nodes at the common interface) of the BEM and FEM meshes are also considered, and this combination is referred here as "node - node".

Table 1: Discretizations for the BEM and FEM sub-domains.

BEM straight constant elements	FEM triangular linear elements
Mesh 1: 20 elements	Mesh 1: 162 elements (20 elements at the interface)
Mesh 2: 40 elements	Mesh 2: 210 elements (40 elements at the interface)
Mesh 3: 80 elements	Mesh 3: 726 elements (80 elements at the interface)
Mesh 4: 160 elements	Mesh 4: 3436 elements (160 elements at the interface)

The relative errors depicted in Figure 4 are computed as follows:

$$\mathrm{E} = \sqrt{\frac{\sum_{i=1}^{\mathrm{nf}}[(|\ {}^{i}\mathrm{U_c}\ |)-(|\ {}^{i}\mathrm{U_a}\ |)]^2}{\sum_{i=1}^{\mathrm{nf}}(|\ {}^{i}\mathrm{U_a}\ |)^2}} \tag{17}$$

where ${}^{i}\mathrm{U_c}$ stands for the computed numerical displacement at point A and frequency i, ${}^{i}\mathrm{U_a}$ stands for the analytical answer at the same point and frequency, and nf is the total number of frequencies considered in the analysis.

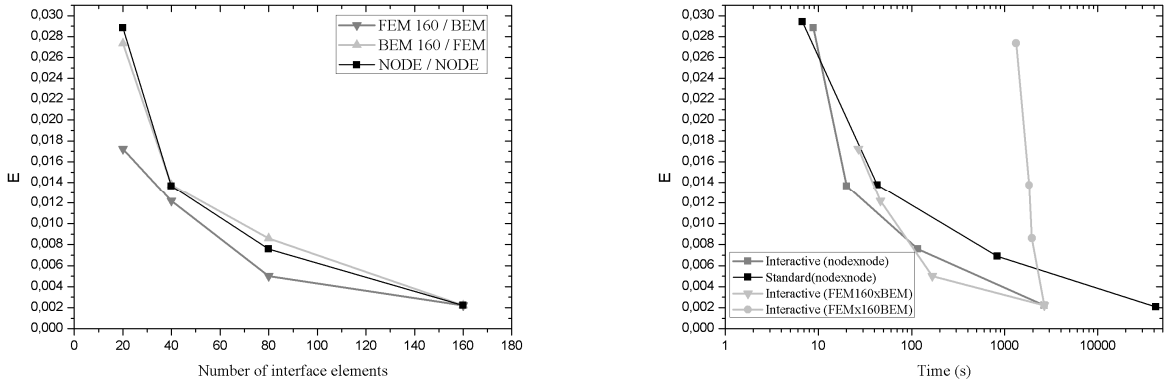

(a) (b)

Figure 4: (a) convergence analysis (error *x* discretization);
(b) efficiency analysis (error *x* CPU time).

As one can observe in Figure 4a, convergence is achieved, even considering non-matching nodes at the common interface. As it can be further observed in Figure 4a, the "BEM 160 / FEM" and the "node / node" curves are very close, indicating that, in this case, a small amount of boundary elements are sufficient to properly discretize the model. On the other hand, better results are obtained considering the "FEM 160 / BEM" combination, which was expected, since refined FEM discretizations can better represent the prescribed boundary conditions of the model, providing more accurate analyses.

In Figure 4b, the computed errors are plotted against the CPU times of the analyses. As one can observe, considering matching nodes at the common interface, the iterative coupling procedure is usually more efficient than the standard direct coupling procedure (i.e., for a given CPU time of analysis, more accurate results can be obtained by the iterative procedure; or, for a given accuracy level, faster analyses can be provided by the iterative procedure). Moreover, as described in Figure 4a, once proper discretizations are considered for each sub-domain of the model, even more efficient analyses may be achieved, highlighting the importance of a coupling procedure that allows flexible and independent discretizations of the involved sub-domains, taking into account non-matching nodes at the common interfaces.

In order to further analyze the performance of the iterative coupling algorithm, the evolution of the optimal relaxation parameter and the convergence of the iterative process are briefly illustrated in Figure 5. In Figure 5a, the total amounts of iterative steps necessary for convergence are depicted, for each frequency, considering the spatial discretizations illustrated in Figure 2. For comparison, results are also depicted considering a constant relaxation parameter value of 0.5. As one can observe, for higher frequencies (above 2500 Hz), convergence is not achieved if $\lambda = 0.5$ is adopted, highlighting the importance of expression (16) for the effectiveness of the iterative coupling analysis. Moreover, for a constant value $\lambda = 1.0$, convergence is never achieved considering the entire adopted frequency range, further illustrating the importance of relaxation parameters in the iterative coupling technique. In Figure 5b, the evolution of the optimally computed relaxation parameters (expression (16)) are illustrated, taking into account $\omega = 5000$ Hz. As one can observe, its evolution is quite complex since it is based on residuals computed at consecutive iterative steps.

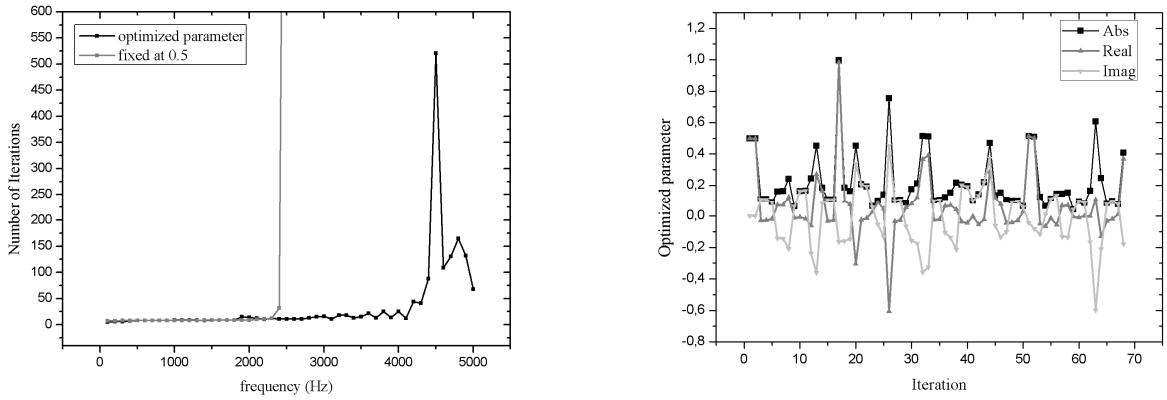

(a) (b)

Figure 5: (a) convergence of the iterative procedure; (b) evolution of the optimal relaxation parameter when $\omega = 5000$ Hz.

6.2 Concrete tunnel surrounded by soil

Consider, once again, a circular homogeneous ring-shaped elastic structure, inside a homogeneous and infinite soil environment. The external environment has a density of 1900 kg/ m^3, Lamé constant $\mu = 2.5 \times 10^{10}$ N/m^2 and Poisson's ratio of 0.35 (no damping). The tunnel structure is made of concrete and has an external radius of 3.0 m and an internal radius of 2.0 m. It has a density of 2500 kg/m^3, Young's modulus of 2.5×10^{10} N/m^2 and Poisson's ratio of 0.2 (no damping). The structure is loaded as indicated in Figure 6a, i.e., the load is applied at the bottom of the concrete ring internal cavity, with constant amplitude of 850 kN/m. The corresponding FEM and BEM discretizations are illustrated in Figure 2b and 2c, respectively. In Figures 6b and 6c, the computed deformation of the tunnel is illustrated, considering $\omega = 500$ Hz.

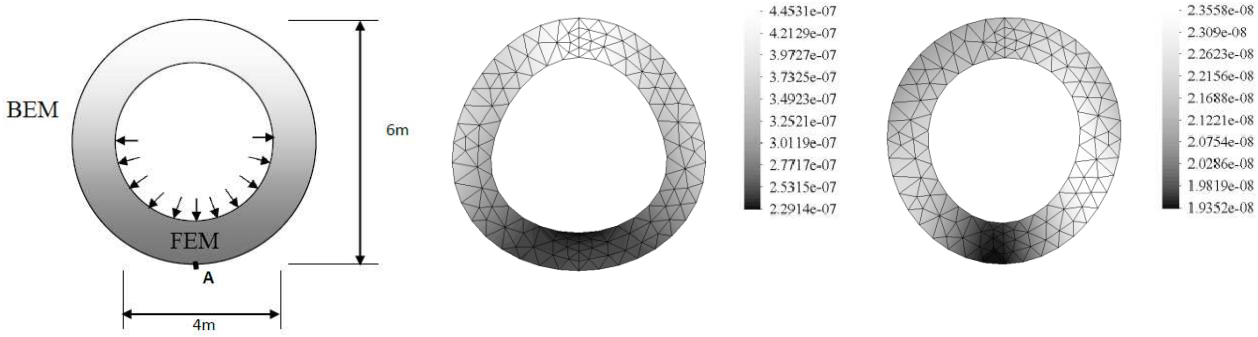

(a) (b) (c)

Figure 6: (a) sketch of the model; and (scaled) deformation of the tunnel for $\omega = 500$ Hz: (b) real part; (c) imaginary part.

Figure 7 illustrates the displacements computed at point A (see Figure 6a), taking into account the proposed iterative and a standard direct FEM-BEM coupling procedure, considering a frequency range from 10 to 500 Hz. As one can observe, the results provided by these different approaches are once again in good agreement, indicating that the iterative solution is converging to the right solution.

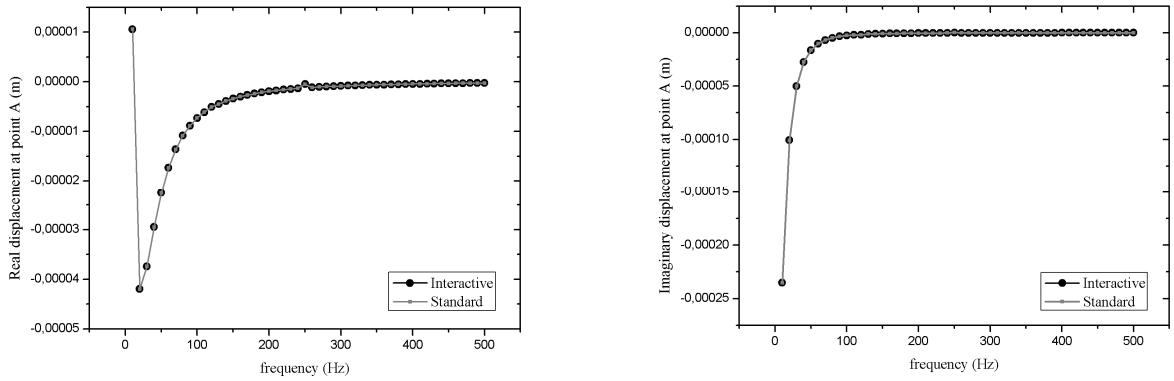

(a) (b)

Figure 7: Vertical displacements at point A: (a) real part; (b) imaginary part.

In Figure 8a, the total amounts of iterative steps necessary for convergence are depicted, taking into account the selected frequency range. As one can note, for all tested frequencies, convergence occurred with a relatively small amount of iterations, with no more than 25 iterations being necessary at any of the tested frequencies. It is important to highlight that, for the present application, for $\lambda = 0.5$ and $\lambda = 1.0$, convergence is never achieved considering the entire adopted frequency range, further illustrating the importance of optimal relaxation parameters in the iterative coupling technique. In Figure 8b, the evolution of the optimally computed relaxation parameters (expression (16)) are illustrated, taking into account $\omega = 430$ Hz.

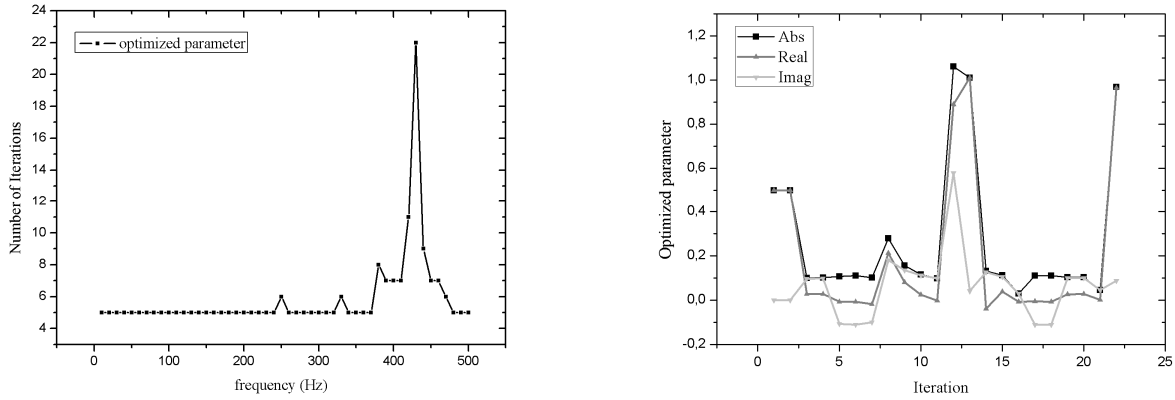

(a) (b)

Figure 8: (a) convergence of the iterative procedure; (b) evolution of the optimal relaxation parameter when $\omega = 430$ Hz.

7 CONCLUSIONS

A FEM-BEM iterative coupling algorithm was discussed here to analyze elastodynamic models, taking into account frequency domain formulations. In order to deal with this ill-posed

problem, optimal relaxation parameters were introduced into the iterative coupling analyses, enabling convergence at a relative low number of iterative steps. An efficient and easy to implement expression to compute the optimal relaxation parameters was discussed and tested, providing an effective and robust iterative coupling procedure.

The use of iterative coupling approaches enables the separated analysis of different sub-domains, leading to better conditioned, smaller and easier to deal with systems of equations, as well as independent definitions of nodal points along distinct sub-domains, allowing non-matching nodes on common interfaces to be easily considered. In section 6 several results were presented, illustrating the versatility and effectiveness of the proposed procedure.

As a matter of fact, the present methodology represents an important step forward in the analyses of wave propagation in frequency domain problems considering iterative coupling procedures, which are well-known ill-posed problems, specially taking into account sub-domains governed by different physical properties and discretized by different numerical techniques.

REFERENCES

[1] Soares Jr. D, von Estorff O, Mansur WJ, (2005), “Efficient nonlinear solid-fluid interaction analysis by an iterative BEM/FEM coupling”, International Journal for Numerical Methods in Engineering, 64, 1416-1431.

[2] Soares Jr. D, (2008), “An optimised FEM-BEM time-domain iterative coupling algorithm for dynamic analyses”, Computers & Structures, 86, 1839-1844.

[3] Warszawski A, Soares Jr. D, Mansur WJ., (2008), “A FEM-BEM coupling procedure to model the propagation of interacting acoustic-acoustic / acoustic-elastic waves through axisymmetric media”, Computer Methods in Applied Mechanics and Engineering, 197, 45-48.

[4] Dominguez J, (1993), Boundary elements in dynamics, Computational Mechanics Publications, Southampton and Boston.

[5] Bathe KJ, (1996), Finite Element Procedures,Prentice Hall Inc., New Jersey.

[6] Hughes TJR, (2000), The Finite Element Method – Linear Static and Dynamic Finite Element Analysis, Dover Publications, New York.

[7] Elleithy WM, Al-Gahtani HJ, El-Gebeily M, (2001), “Iterative coupling of BE and FE methods in elastostatics”, Engineering Analysis with Boundary Elements, 25, 685–695.